Published in final edited form as:
J Immunol. 2011 December 1; 187(11): 5568–5576. doi:10.4049/jimmunol.1102104.

Quantifying antigen-specific CD4 T cells during a viral infection: CD4 T cell responses are larger than we think

Daniel S. McDermott[*] and **Steven M. Varga**[*,†,‡]

[*]Interdisciplinary Graduate Program in Immunology, University of Iowa, Iowa City, IA 52242, USA

[†]Department of Pathology, University of Iowa, Iowa City, IA 52242, USA

[‡]Department of Microbiology, University of Iowa, Iowa City, IA 52242, USA

Abstract

The number of virus-specific CD8 T cells increases substantially during an acute infection. Up to 90% of CD8 T cells are virus-specific following lymphocytic choriomeningitis virus (LCMV) infection. In contrast, studies identifying virus-specific CD4 T cell epitopes have indicated that CD4 T cells often recognize a broader array of antigens than CD8 T cells consequently making it difficult to accurately quantify the total magnitude of pathogen-specific CD4 T cell responses. Here we show that following LCMV infection CD4 T cells become CD11a^{hi}CD49d^{+} and retain this expression pattern into memory. During the effector phase, all of the LCMV-specific IFN-γ^{+} CD4 T cells display a CD11a^{hi}CD49d^{+} cell surface expression phenotype. In addition, only memory CD11a^{hi}CD49d^{+} CD4 T cells make IFN-γ following stimulation. Furthermore, upon secondary LCMV challenge, only CD11a^{hi}CD49d^{+} memory CD4 T cells from LCMV-immune mice undergo proliferative expansion, demonstrating that CD11a^{hi}CD49d^{+} CD4 T cells are truly Ag-specific. Using the combination of CD11a and CD49d, we demonstrate that up to 50% of the CD4 T cells are virus-specific during the peak of the LCMV response. Our results indicate that the magnitude of the virus-specific CD4 T cell response is much greater than previously recognized.

Keywords

Lung; Rodent; T cells; Viral

Introduction

CD4 T cells play a vital role in coordinating adaptive immune responses during viral infection. However, a number of factors conspire to make it difficult to quantify virus-specific CD4 T cell responses. During viral infections, CD4 T cells specific for known epitopes accumulate at much lower numbers than their CD8 T cell counterparts. Additionally, in contrast to CD8 T cells that maintain a stable memory population, the number of memory CD4 T cells gradually decreases over time (1). Furthermore, activated CD4 T cells can differentiate into one of a number of subsets that have unique cytokine production signatures making the identification of Ag-specific CD4 T cells based solely on cytokine release more difficult (1, 2). Two common methods used to identify pathogen-specific effector and/or memory CD4 T cells are *in vitro* peptide stimulation followed by

Address of correspondence and reprint request to Dr. Steven Varga, Department of Microbiology, 51 Newton Road, 3-532 B.S.B., University of Iowa, Iowa City, IA 52242. steven-varga@uiowa.edu.

Disclosures
The authors have no financial conflict of interest.

intracellular cytokine staining (ICS) or MHC class II tetramer staining (3, 4). However, both require prior knowledge regarding the Ag specificity of the CD4 T cells (4). Moreover, recent studies aimed at identifying pathogen-specific CD4 T cell epitopes have indicated that CD4 T cells often recognize a broad array of pathogen-encoded proteins resulting in a low frequency of CD4 T cells specific to any individual epitope. Taken together, the above obstacles have prevented accurate quantification of the magnitude of pathogen-specific CD4 T cell responses (5).

Recent studies have demonstrated that following lymphocytic choriomeningitis virus (LCMV) infection Ag-specific CD8 T cells downregulate the cell surface expression of CD8α and increase expression of the trafficking molecule CD11a (6, 7). Importantly the magnitude of pathogen-specific CD8 T cell responses can now be determined using this technique without prior knowledge of the Ag specificity of the responding CD8 T cells. However, no analogous technique is currently available to estimate the magnitude of the Ag-specific CD4 T cell response following viral infection. Activated CD4 T cells downregulate CD62L and CCR7 expression allowing for their egress from lymph nodes (8, 9). These activated CD4 T cells subsequentely upregulate cell surface expression of integrins such as $\alpha_4\beta_1$ (CD49d and CD29, respectively) and $\alpha_L\beta_2$ (CD11a and CD18, respectively) that mediate their migration to the site of infection (8, 9). Therefore, given the important role of integrins in the migration of effector CD4 T cells, we sought to determine if modulation of these trafficking molecules would provide a reliable cell surface phenotypic profile to identify Ag-specific CD4 T cells following viral infection.

In this study, we demonstrate that LCMV-specific CD4 T cells increase cell surface expression of CD11a and induce expression of CD49d following infection and that expression of these molecules remains stable into memory. We show that whereas naïve CD4 T cells are $CD11a^{lo}CD49d^{-}$, LCMV-specific effector CD4 T cells identified by LCMV-peptide-driven IFN-γ production are $CD11a^{hi}CD49d^{+}$. In addition, we demonstrate that only $CD11a^{hi}CD49d^{+}$ CD4 T cells from LCMV-immune mice produce IFN-γ following stimulation and that only $CD11a^{hi}CD49d^{+}$ CD4 T cells from LCMV-immune mice respond following a secondary LCMV challenge. Our results demonstrate that the combination of CD11a and CD49d can be used to determine the magnitude of the Ag-specific CD4 T cell response following infection and that all LCMV-specific memory CD4 T cells are $CD11a^{hi}CD49d^{+}$. Importantly, we demonstrate that up to 50% of the CD4 T cells at the peak of the LCMV response are $CD11a^{hi}CD49d^{+}$, indicating that the magnitude of the Ag-specific CD4 T cell response following viral infection is much greater than previously recognized.

Materials and Methods

Mice and viruses

BALB/cAnNCr, C57BL/6NCr, B6-Ly5.2/Cr and outbred Swiss Webster mice between 6 and 8 weeks of age were purchased from the National Cancer Institute (NCI; Frederick, MD). C57BL/6 SMARTA TCR-transgenic (Tg) mice (10) were a gift from Michael J. Bevan (University of Washington, Seattle, WA). Female mice were used in all experiments. The Armstrong strain of LCMV and Pichinde virus (PV) were gifts from Raymond M. Welsh (University of Massachusetts Medical School, Worcester, MA) and were both propagated on BHK-21 cells (American Type Culture Condition; ATCC, Manassas, VA) (11). The Western Reserve strain of vaccinia virus (VACV) was also a gift from Raymond M. Welsh and was propagated on BSC-40 cells (ATCC) (11). The A2 strain of respiratory syncytial virus (RSV) was a gift from Barney S. Graham (National Institutes of Health, Bethesda, MD) and was propagated on HEp-2 cells (ATCC) (12). All experimental

procedures utilizing mice were approved by the University of Iowa Animal Care and Use Committee.

Adoptive Transfer of SMARTA CD4 T cells

SMARTA CD4 T cells (1×10^4) were adoptively transferred i.v. into naive C57BL/6 mice. 24 h post-transfer, recipient C57BL/6 mice were infected intranasally (i.n.) with 5×10^5 PFU LCMV (13). Spleen and lungs were harvested at days 8 and 30 post-infection. Lung mononuclear cells were isolated as previously described (12). Cells were stained with mAbs specific to CD4 and CD90.2 as well as to either CD11a, CD29, CD44, CD49b, CD49d, CD49e, CD54, CD62L, CD90.1, CD103 or PSGL-1 (eBioscience, Inc, San Diego, CA) and analyzed on aBD FACSCanto (BD Bioscience, San Jose, CA) as previously described (12). Data were analyzed using FlowJo software (Tree Star Inc, Ashland, OR).

In some experiments, SMARTA CD4 T cells ($2–3\times10^6$) were adoptively transferred i.v. into naive C57BL/6 mice and recipient mice were infected i.p. 24 hours later with either 5×10^5 PFU LCMV, 1×10^6 PFU PV, or 100 μg CpG. Spleens were harvested at day 8 post-infection (11) and splenocytes were stained with mAbs specific to CD4, CD11a, CD49d and CD90.1 and subsequently analyzed on aBD FACSCanto. To purify $CD11a^{hi}CD49d^{+}$ and $CD11a^{lo}CD49d^{-}$ CD4 T cells, splenocytes from day ≥60 LCMV-immune B6-Ly5.2/Cr ($CD45.1^{+}$) mice were stained with CD4-APC-Cy7 (Biolegend, San Diego, CA). Cells were subsequently stained with anti-Cy7 magnetic beads (Miltenyi Biotec Inc, Auburn, CA) and positively selected using an AutoMACS (Miltenyi Biotec). AutoMACS-enriched cells were stained for CD90.2, CD49d and CD11a and sorted using a BD FACSAria II (BD Biosciences). Sorted populations were labeled with CFSE (Molecular Probes, Carlsbad, CA) and 1.2×10^5 CFSE-labeled cells were adoptively transferred i.v. into C57BL/6 ($CD45.2^{+}$) mice.

RSV infection

BALB/c mice were infected i.n. with 3.1×10^6 PFU RSV. Lung and bronchoalveolar lavage (BAL) mononuclear cells were isolated and stained with with mAbs specific to CD4, CD11a, CD49d and CD90.2 as previously described (14). Cells were analyzed on a BD FACSCanto flow cytometer and data were analyzed using FlowJo software.

Intracellular cytokine stain

Spleen and lung cells from LCMV-infected mice and lung cells from RSV-infected mice were incubated with either 1 μM of the LCMV-derived peptide $GP_{66–80}$ (5, 15) (Biosythesis, Inc, Lewisville, TX) or the RSV-derived peptides $G_{183–195}$ or $F_{51–66}$ (16–18), respectively, in the presence of 10 μg/ml brefeldin A (BFA; Sigma-Aldrich Corp, St. Louis, MO) for 5 h at 37°C (5, 13). PBL from LCMV-immune mice were stimulated with 50 ng/ml PMA (Sigma-Aldrich), and 500 ng/ml ionomycin (Sigma-Aldrich) in the presence of 10 mg/ml brefeldin A for 3.5 h at 37°C (19). Following stimulation, cells were surfaced-stained with mAbs specific to CD4, CD11a, CD49d and CD90.2. Intracellular staining for IFN-γ was performed as previously described (13). Cells were analyzed on aBD FACSCanto flow cytometer and data were analyzed using FlowJo software.

Results

Alterations in CD11a and CD49d cell surface expression on virus-specific Tg-CD4 T cells following acute LCMV infection

The magnitude of pathogen-specific CD8 T cell responses can be determined through the use of the surrogate activation markers $CD8^{lo}CD11a^{hi}$ (6, 7). We sought to develop a similar strategy to identify Ag-experienced CD4 T cells in order to quantify the magnitude of

pathogen-specific CD4 T cell responses. Previous studies have demonstrated that *Salmonella*-specific CD4 T cells are CD11a^{hi} (20). However, following viral infection CD11a expression decreases on memory CD4 T cells making it difficult to distinguish naive from memory CD4 T cells based solely on CD11a expression. Furthermore, in contrast to CD8 T cells, CD4 T cells do not modulate CD4 expression. Therefore we sought to find additional markers in order to more easily identify Ag-specific CD4 T cells.

Activated CD4 T cells utilize various integrins to traffic to sites of inflammation following infection (8, 9), therefore we sought to determine if modulation of integrins would provide a reliable cell surface phenotypic profile to identify Ag-specific CD4 T cells. We utilized an adoptive transfer model to examine the cell surface expression of several trafficking molecules following acute LCMV infection. 1×10^4 LCMV-specific SMARTA CD4 T cells (CD90.1$^+$) were adoptively transferred into naive C57BL/6 mice (CD90.2$^+$), followed 24 hours post-transfer by i.n. LCMV infection, mimicking the natural route of LCMV infection. At both acute and memory timepoints (i.e. day 8 and 30, respectively) we analyzed the cell surface expression of a wide range of integrins and adhesion molecules on gated SMARTA cells from the spleen (Figure 1A) and lung (Figure 1B). At both timepoints, CD4 T cells from the spleen and lung exhibited increased expression of the memory marker CD44 as compared to CD4 T cells obtained from the spleen and lung of naïve SMARTA mice (Figure 1). In addition, we observed increased expression of the adhesion molecules CD11a, CD49d and CD29 on both acute and memory CD4 T cells from the spleen (Figure 1A) and lung (Figure 1B) in comparison to naïve SMARTA cells. Several additional markers were examined (i.e. CD62L, CD54, β7 integrin, CD49b (DX-5), CD49e, CD49f, CD103, PSGL-1, CD45RB, and Ly6C), however, the majority of CD4 T cells did not exhibit altered cell surface expression of these molecules at either acute or memory timepoints (Figure 1). These data suggest that following LCMV infection, LCMV-Tg CD4 T cells upregulate the cell surface expression of CD11a, CD49d, CD29 and CD44 and retain this expression pattern into memory.

Changes in CD11a and CD49d cell surface expression on endogenous CD4 T cells following acute LCMV infection

We next asked if modulation of integrins could be used to distinguish naïve from activated CD4 T cells within the endogenous CD4 T cell population following acute LCMV infection. To address this question, we examined cell surface expression of CD11a in combination with either CD49d, CD29 or CD44 on endogenous (CD4$^+$CD90.1$^-$) splenic (Figure 2A) and lung (Figure 2B) CD4 T cells following LCMV infection. We found that CD11a in combination with all three markers allowed for the clear discrimination of the activated endogenous CD4 T cells from naïve CD4 T cells during both acute and memory time points. However, the fraction of CD11a^{hi}CD49d$^+$ CD4 T cells from naïve mice was substantially lower than that of either the CD11a^{hi}CD44$^+$ or CD11a^{hi}CD29$^+$ populations (Figure 2). Therefore we focused on the combined expression of CD11a and CD49d for the remainder of our studies. Importantly, at day 8 post-LCMV-infection approximately 40% of the CD4 T cells in the spleen and 50% in the lung were CD11a^{hi}CD49d$^+$, suggesting that the magnitude of the LCMV-specific CD4 T cell response is much larger than what has been previously demonstrated using *in vitro* peptide stimulation followed by either ICS or ELISPOT analysis for IFN-γ production (5, 21–23).

Increased CD11a and CD49d cell surface expression requires interaction with cognate Ag

Infections induce both T cell receptor signals and inflammatory cytokines, either of which could alter the expression of integrins. To determine if modulation of CD11a and CD49d cell surface expression requires TCR interaction with cognate Ag, we adoptively transferred naïve SMARTA CD4 T cells into naïve C57BL/6 mice. Recipient mice were subsequently

administered either 100 μg CpG or 1×10^6 PFU PV to induce a non-specific inflammatory environment. Additional recipients received either PBS or LCMV as a negative and positive control, respectively. Spleens were harvested 8 days later and we examined CD11a and CD49d expression on the transferred SMARTA CD4 T cells (Figure 3). SMARTA cells isolated from either CpG-treated or PV-infected animals displayed no increase in the cell surface expression of CD11a and CD49d as compared to the PBS control mice (Figure 3). However, SMARTA cells obtained from LCMV-infected mice demonstrated a significant ($p<0.001$) upregulation of CD11a and CD49d. These data show that Ag stimulation is required to cause increased cell surface expression of CD11a and induce cell surface expression of CD49d on CD4 T cells and that expression of these molecules is not modulated by nonspecific inflammation generated by either a TLR agonist or a heterologous viral infection.

CD11a^{hi}CD49d^{+} effector CD4 T cells are Ag-specific

We have demonstrated that the cell surface expression of CD11a and CD49d are modulated on CD4 T cells following LCMV infection, however, we next wanted to determine if these CD11a^{hi}CD49d^{+} CD4 T cells are truly Ag-specific. In order to confirm that CD11a^{hi}CD49d^{+} CD4 T cells represent Ag-specific cells, spleens and lungs were harvested from LCMV-infected C57BL/6 mice at the peak of infection (i.e. day 8), followed by *in vitro* peptide stimulation with the LCMV-specific CD4 T cell immunodominant epitope $GP_{66–80}$ (5, 15). When IFN-γ-production from CD11a^{hi}CD49d^{+} CD4 T cells vs. CD11a^{lo}CD49d$^{−}$ CD4 T cells was compared, we observed that essentially all of the IFN-γ-producing CD4 T cells in the spleen and lung were CD11a^{hi}CD49d^{+} (98.0% and 98.7%, respectively; Figure 4A and B). These data demonstrate that LCMV-specific effector CD4 T cells are CD11a^{hi}CD49d^{+}. Furthermore, the above data indicate that 40–50% of the CD4 T cells during acute LCMV infection are virus-specific.

We further tested whether or not CD11a and CD49d expression patterns could distinguish naïve from Ag-experienced CD4 T cells following acute RSV infection. Similar to LCMV infection, CD4 T cells in the lung and BAL upregulated CD11a and CD49d cell surface expression following acute RSV infection (Figure 5A; Day 8). Although CD4 T cells in the lung parenchyma remain CD11a^{hi}, at day 15 post-infection, CD4 T cells within the lung airways display downregulated expression of CD11a as previously described (24). However, unlike CD11a, CD49d expression was not decreased on CD4 T cells in the lung airways, suggesting that CD49d is sufficient to distinguish Ag-specific cells within the lung airways following at least day 15 post-infection. To determine if the CD11a^{hi}CD49d^{+} CD4 T cells in the lung and the lung airways are RSV-specific, we utilized *in vitro* peptide stimulation followed by ICS to identify RSV-specific CD4 T cells and examined IFN-γ-production from CD11a^{hi}CD49d^{+} CD4 T cells vs. CD11a^{lo}CD49d$^{−}$ CD4 T cells. RSV $G_{183–195}$- (16, 17) and RSV $F_{51–66}$-specific (18) lung CD4 T cells were CD11a^{hi}CD49d^{+} (Figure 5B), demonstrating that the cell surface upregulation of CD11a and CD49d on Ag-experienced effector CD4 T cells occurs during other viral infections.

CD11a^{hi}CD49d^{+} memory CD4 T cells are Ag-specific

Having established that effector CD4 T cells are CD11a^{hi}CD49d^{+}, we next asked if CD11aand CD49d cell surface expression can be used to identify LCMV-specific memory CD4 T cells. To address this question we sorted CD11a^{hi}CD49d^{+} and CD11a^{lo}CD49d$^{−}$ CD4 T cells from LCMV-immune (i.e. day ≥60 post-LCMV infection) CD45.1^{+} congenic mice, CFSE-labeled the sorted cells and subsequently adoptively transferred them into naive CD45.2^{+} recipients. Recipient mice were either infected with LCMV or given PBS as a control and the CFSE dilution profiles of the transferred cells isolated from the spleen were examined at day 4 post-infection. CD11a^{lo}CD49d$^{−}$ CD4 T cells did not proliferate in either

control PBS or LCMV-infected mice (Figure 6A). In contrast, CD11a^{hi}CD49d^{+} CD4 T cells proliferated vigorously upon LCMV infection, but did not proliferate in PBS control animals (Figure 6B). To further confirm that CD11a^{hi}CD49d^{+} CD4 T cells within LCMV-immune mice are truly LCMV-specific cells, we stimulated CD4 T cells from the PBL of LCMV-immune mice and examined IFN-γ production. When IFN-γ-production from CD11a^{hi}CD49d^{+} CD4 T cells vs. CD11a^{lo}CD49d^{-} CD4 T cells was compared, we observed that essentially all of the IFN-γ-producing CD4 T cells in the PBL of LCMV-immune mice were CD11a^{hi}CD49d^{+} (~98%; Figure 6C). Together, these data indicate that all of the Ag-specific memory CD4 T cells are CD11a^{hi}CD49d^{+}. Taken together our results show that cell surface expression of CD11a and CD49d can be used to identify Ag-specific CD4 T cells over the course of an infection.

The magnitude and kinetics of the Ag-specific CD4 T cell response following infection

Our data indicates that Ag-specific CD4 T cells can be tracked in inbred populations following viral infection using CD11a and CD49d. We next sought to determine if CD11a and CD49d expression patterns could be used to track Ag-specific CD4 T cells within an outbred population. C57BL/6, BALB/c and outbred Swiss Webster mice were infected with LCMV and CD4 T cells were examined in the blood at various timepoints following infection (Figure 7). Few CD11a^{hi}CD49d^{+} CD4 T cells were present in the PBL of any of the strains until day 6. LCMV infection of C57BL/6 mice resulted in a large expansion of CD11a^{hi}CD49d^{+} CD4 T cells that peaked uniformly at day 8 post-infection (56.6±4.6%; Figure 7A). In contrast, LCMV infection of BALB/c mice resulted in a relatively low frequency of CD11a^{hi}CD49d^{+} CD4 T cells that peaked at day 10 post-infection (14.9±3.3%; Figure 7B). The peak frequency of CD11a^{hi}CD49d^{+} CD4 T cells in Swiss Webster mice was less uniform than in the inbred strains (43.4±9.5%; Figure 7C), similar to what has been previously reported for CD8 T cells during LCMV infection (6). Although the peak frequency of CD11a^{hi}CD49d^{+} CD4 T cells varied, the overall kinetics of the CD4 T cell response in the outbred strain was similar between each individual mouse, with the majority of mice exhibiting a peak at day 10 post-infection (Figure 7C). Overall these data demonstrate that the genetic background can have a substantial effect on the overall kinetics and magnitude (i.e. C57BL/6 mice vs. BALB/c) of the CD4 T cell response following infection with the same virus. Furthermore, these data demonstrate that although outbred hosts display similar overall CD4 T cell expansion and contraction kinetics following infection, there is a large degree of variability in the total magnitude of the CD4 T cell response within an outbred host population.

The kinetics of the CD4 T cell response in immune mice following heterologous infection

Our data indicate that the increase of CD11a cell surface expression combined with the induction of CD49d expression following infection can be used to track Ag-specific CD4 T cells. However, the above experiments examined naïve mice infected with a single pathogen in contrast to hosts that would have a previous infection history. Therefore, we sought to determine if CD11a and CD49d can be used to track newly activated CD4 T cells in an animal that has been previously exposed to other pathogens. We infected naïve mice with VACV on day 0 (Day 0 VACV) and tracked the CD11a^{hi}CD49d^{+} CD4 T cells throughout the acute infection (Figure 8). At day 35 post-infection, we infected the VACV-immune mice, as well as additional age-matched naïve mice (LCMV only) with LCMV. At the time of infection, ~2.5% of the CD4 T cells from the naïve mice were CD11a^{hi}CD49d^{+}, whereas, due to the presence of virus-specific memory CD4 T cells, ~6.5% of the CD4 T cells in the VACV-immune mice were CD11a^{hi}CD49d^{+}. Importantly, at the peak of the LCMV infection (i.e. day 43; day 8 post-LCMV infection), the total magnitude of the primary LCMV-specific CD4 T cell response (i.e. newly generated CD11a^{hi}CD49d^{+} CD4 T cells) in the VACV-immune and LCMV only mice was ~46% (Figure 8). Furthermore, the frequency

of LCMV-specific memory cells (i.e. day 70; day 35 post-LCMV infection) was ~6.5%, indicating that CD11a and CD49d cell surface expression can be utilized to track newly generated memory cells following a heterologous infection. These results indicate that, as long as the baseline frequency of the $CD11a^{hi}CD49d^{+}$ memory CD4 T cells within a host is known, that the kinetics of a newly generated Ag-specific CD4 T cell response can be accounted for using CD11a and CD49d surface expression.

Discussion

Virus-specific CD8 T cell responses have been extensively examined. However, a number of obstacles hamper the analysis of virus-specific CD4 T cells. Several epitope mapping studies have indicated that CD4 T cell epitopes are commonly spread throughout the entire viral proteome and quantitation using immundominant epitopes often accounts for only a small percentage of the activated CD4 T cells (5, 11, 25, 26). These combined factors make studying the CD4 T cell response using common methods such as ICS or ELISPOT following *in vitro* peptide stimulation or MHC Class II tetramers difficult. Therefore in these studies, we set out to identify potential cell surface markers that would reliably identify Ag-specific CD4 T cells following a viral infection.

Here we demonstrate that upon acute LCMV infection, LCMV-Tg SMARTA CD4 T cells increase the cell surface expression of CD11a and induce expression of CD49d (Figure 1). Expression of these integrins remains increased on memory CD4 T cells as compared to naïve SMARTA CD4 T cells (Figure 1). To determine if these markers are modulated in a similar manner on a polyclonal population of CD4 T cells, we examined the cell surface expression pattern of CD11a and CD49d on endogenous CD4 T cells following LCMV infection. We show that following acute LCMV infection, endogenous CD4 T cells from both the spleen and lungs, like SMARTA CD4 T cells, are $CD11a^{hi}CD49d^{+}$ and that these cells remain $CD11a^{hi}CD49d^{+}$ into memory (Figure 2). It is important to note that several previous studies have reported the increased cell surface expression of CD11a or the induction of CD49d expression on acute and memory CD4 T cells following infection. For example, previous studies have noted the induced expression of CD49d (i.e. VLA-4) on CD4 T cells following LCMV infection and that memory LCMV-specific CD4 T cells exhibit increased cell surface CD11a expression (27, 28). In addition, studies examining CMV-specific CD4 T cells following both acute and latent CMV infection reported induced cell surface expression of CD49d as well as increased cell surface expression of CD11a (29). Furthermore, CD11a cell surface expression is increased on acute and memory CD4 T cells following infection with recombinant VACV, as well as following *Salmonella* infection (20, 25) and Sendai virus-specific memory CD4 T cells express high levels of CD49d (28, 30). These studies further substantiate our data indicating that the combined use of CD11a and CD49d cell surface expression patterns can be utilized to track antigen-specific CD4 T cells following viral infections.

Although we demonstrate that CD11a and CD49d expression patterns can be used to track Ag-specific CD4 T cells at the peak of the response and into memory, it is important to note that there may be limitations to utilizing these markers during the early stages of infection (i.e. prior to day 4.5 post-infection). Previous studies have shown that following influenza virus infection transferred naïve CFSE-labeled influenza-specific TCR-Tg CD4 T cells express high levels of CD49d only after undergoing at least 6 cell divisions (31). Furthermore, other reports demonstrate that following OVA injection, OVA-specific DO11.10 CD4 T cells from the lymph nodes upregulate CD49d surface expression only after 5–6 cell divisions (32). Following LCMV infection, LCMV-specific SMARTA CD4 T cells do not undergo proliferation during the first two days of infection, however by day 3 these cells have begun to undergo extensive proliferation and by day 4 CFSE is completely

diluted (33), suggesting that CD11a and CD49d can be used to reliably track Ag-specific CD4 T cells following day 4 post-infection. Consistent with this conclusion, we observed that SMARTA CD4 T cells do not induce CD49d cell surface expression until day 4 post-LCMV infection, whereas we observe increased expression of CD11a by this time (data not shown). Taken together, the above studies suggest the CD11a and CD49d cell surface expression patterns can be utilized to track Ag-specific CD4 T cells starting at least by day 4 post-viral infection.

We demonstrate that modulation of CD11a and CD49d expression requires the presence of cognate Ag and is not altered due to either TLR stimulation or the inflammatory environment created by PV (Figure 3). Importantly, virtually all of the GP66–80-specific CD4 T cells, as measured by either IFN-γ production following *in vitro* peptide stimulation or tetramer staining are $CD11a^{hi}CD49d^{+}$ (Figure 4 and data not shown). Interestingly, following *in vitro* peptide stimulation using GP66–80, which accounts for greater than 90% of the total LCMV-response to known epitopes (data not shown), we are only able to account for 20–30% of the total $CD11a^{hi}CD49d^{+}$ CD4 T cell population. Similarly, PMA/Ionomycin stimulation of LCMV-specific memory CD4 T cells only induces IFN-γ production from ~55% of the $CD11a^{hi}CD49d^{+}$ CD4 T cells (Figure 6B). In an effort to account for all of the $CD11a^{hi}CD49d^{+}$ LCMV-specific CD4 T cells we stimulated splenic and lung CD4 T cells with LCMV-infected dendritic cells. Interestingly, we observe a similar percentage of IFN-γ-producing splenic CD4 T cells following stimulation with LCMV-infected dendritic cells compared to stimulation with control GP66–80 pulsed dendritic cells (~7.5%; data not shown). A similar discrepancy has been previously described in the VACV model, in which ~20% of the CD4 T cells express CD11a whereas when stimulated with VACV-infected A20 B cells, only ~3% of the CD4 T cells produced IFN-γ (25). Furthermore, previous studies have demonstrated that only 50–60% SMARTA LCMV-Tg CD4 T cells produce IFN-γ following stimulation with the peptide GP61–80, suggesting that a large fraction of the Ag-specific effector CD4 T cells do not produce cytokine upon restimulation with their cognate Ag (33). These studies suggest that the use of CD11a and CD49d may provide a more accurate means to quantify of the magnitude of the CD4 T cell response than can be obtained by examination of cytokine responses.

Additionally, we demonstrate that effector CD4 T cells from the lung and BAL upregulate cell surface levels of CD11a and CD49d following acute RSV infection (Figure 5A), indicating the usefulness of this approach in multiple infection models. Furthermore, virtually all of the $IFN\text{-}\gamma^{+}$ CD4 T cells following G183–195 and F51–66 stimulation are $CD11a^{hi}CD49d^{+}$ (Figure 5B) demonstrating that the RSV-specific CD4 T cells exhibit a $CD11a^{hi}CD49d^{+}$ expression pattern. However, it is important to note that CD4 T cells from the BAL exhibit decreased cell surface expression of CD11a by day 15 post-RSV infection, but still retain CD49d expression (Figure 5A). Downregulation of CD11a expression by memory CD4 T cells in the BAL has been previously described (24), however the mechanism or biological significance of decreased CD11a expression in the lung airways is currently unclear. In contrast, we demonstrate that CD49d cell surface expression does not decrease on memory CD4 T cells in the lung airway by day 15 (Figure 5A). Furthermore, preliminary data from our laboratory suggests that the majority of CD4 T cells (~80%) from the BAL at day 30 still exhibit cell surface expression of CD49d (data not shown), thus indicating that CD49d expression, but not CD11a, can be utilized to track memory CD4 T cells within the lung airways.

Similar to the LCMV-specific effector CD4 T cells, we show that all LCMV-specific memory CD4 T cells are $CD11^{hi}CD49d^{+}$, as sorted $CD11^{hi}CD49d^{+}$ but not $CD11^{lo}CD49d^{-}$ CD4 T cells from LCMV-immune mice proliferate upon secondary LCMV infection (Figure 6A and 6B). Furthermore, virtually all of the IFN-γ producing cells from LCMV-immune

mice are $CD11a^{hi}CD49d^{+}$ (Figure 6C). Furthermore, we demonstrate that upon heterologous challenge of VACV-infected mice with LCMV, at the peak of infection the overall magnitude of the primary LCMV-specific CD4 T cell response (i.e. newly activated $CD11a^{hi}CD49d^{+}$ CD4 T cells) is similar to LCMV-infected naïve mice at the peak of the response (~45%) and into memory (~6.5 %; Figure 8). These data indicate that CD11a and CD49d can be used to track memory virus-specific CD4 T cells, as well as newly generated virus-specific CD4 T cells in an animal that has been previously exposed to a different pathogen as long as the baseline frequency of $CD11a^{hi}CD49d^{+}$ CD4 T cells is known prior to infection. These data are important in the context of the potential use of CD11a and CD49d expression patterns to track Ag-specific CD4 T cell responses in human hosts that have likely been exposed to numerous pathogens prior to examination. Interestingly, a recent study has demonstrated that activated, cytokine-producing human CD4 T cells are $CD49d^{+}$ (34). Furthermore, naïve human CD4 T cells are $CD11a^{lo}$ and become $CD11a^{hi}$ upon activation and retain elevated CD11a expression into memory (26). Taken together, these studies suggest that the combination CD11a and CD49d may be a useful tool to examine the kinetics and magnitude of CD4 T cell responses following either vaccination or infection in humans.

Although several studies have previously noted the expression of CD11a or CD49d on either activated or memory CD4 T cells following infection (20, 24, 28–32), here we demonstrate for the first time that CD11a and CD49d can be used in combination to track Ag-specific CD4 T cells following viral infection. Previous studies examining the magnitude of the CD4 T cell response in C57BL/6 mice following LCMV infection have shown that ~10% of CD4 T cells at the peak of LCMV infection are virus-specific (5, 21, 23). In contrast, our analyses measuring changes in cell surface expression patterns of CD11a and CD49d demonstrates that up to 50% of the CD4 T cells are virus-specific at the peak of the LCMV-induced immune response, indicating that the magnitude of the Ag-specific CD4 T cell response is much greater than previously recognized. It is important to note that while over 50% of the CD4 T cells following LCMV infection of C57BL/6 mice are Ag-specific, only ~15% of the CD4 T cells within BALB/c mice were Ag-specific (Figure 7). These data, along with the large degree of variability observed within the outbred Swiss Webster mice following LCMV infection, suggest that the genetic background of the animal greatly controls the magnitude and kinetics of the CD4 T cell response. Interestingly, similar results have been described for CD8 T cells following infection with *Listeria monocytogenes* (6). Much recent work has focused on determining the Ag-specificity of CD4 T cells against LCMV and other viruses in different strains of mice. However, until now no technique has been available to accurately quantify the total number of virus-specific CD4 T cells.

We believe that the combined use of CD11a and CD49d will grant, for the first time, the ability to accurately track the kinetics and magnitude of the entire endogenous CD4 T cell response from the expansion phase into memory. Importantly, we show that CD11a and CD49d cell surface expression patterns can be used to track virus-specific CD4 T cells in outbred populations. These data suggest the potential in using the modulation of CD11a and CD49d expression to verify vaccine-induced responses by determining the magnitude of Ag-specific CD4 T cell responses in humans following immunization.

Acknowledgments

We thank John Harty for critical review of the manuscript and Stacey Hartwig for technical assistance.

This work was supported by National Institutes of Health Grant R01 AI063520 to S.M.V. and the Predoctoral Training Program in Immunology Grant T32 AI007485 to D.S.M.

Abbreviations in this paper

ICS	intracellular cytokine staining
Tg	transgenic
LCMV	lymphocytic choriomeningitis virus
PV	Pichinde virus
VACV	vaccinia virus
RSV	respiratory syncytial virus
i.n	intranasal
BAL	bronchoalveolar lavage
BFA	brefeldin A

References

1. Seder RA, Ahmed R. Similarities and differences in $CD4^+$ and $CD8^+$ effector and memory T cell generation. Nat Immunol. 2003; 4:835–842. [PubMed: 12942084]
2. Whitmire JK. Induction and function of virus-specific $CD4^+$ T cell responses. Virology. 2011
3. Jenkins MK, Khoruts A, Ingulli E, Mueller DL, McSorley SJ, Reinhardt RL, Itano A, Pape KA. In vivo activation of antigen-specific CD4 T cells. Annu Rev Immunol. 2001; 19:23–45. [PubMed: 11244029]
4. MacLeod MK, Clambey ET, Kappler JW, Marrack P. CD4 memory T cells: what are they and what can they do? Semin Immunol. 2009; 21:53–61. [PubMed: 19269850]
5. Dow C, Oseroff C, Peters B, Nance-Sotelo C, Sidney J, Buchmeier M, Sette A, Mothe BR. Lymphocytic choriomeningitis virus infection yields overlapping $CD4^+$ and $CD8^+$ T-cell responses. J Virol. 2008; 82:11734–11741. [PubMed: 18829752]
6. Rai D, Pham NL, Harty JT, Badovinac VP. Tracking the total CD8 T cell response to infection reveals substantial discordance in magnitude and kinetics between inbred and outbred hosts. J Immunol. 2009; 183:7672–7681. [PubMed: 19933864]
7. Masopust D, Murali-Krishna K, Ahmed R. Quantitating the magnitude of the lymphocytic choriomeningitis virus-specific CD8 T-cell response: it is even bigger than we thought. J Virol. 2007; 81:2002–2011. [PubMed: 17151096]
8. Springer TA. Traffic signals for lymphocyte recirculation and leukocyte emigration: the multistep paradigm. Cell. 1994; 76:301–314. [PubMed: 7507411]
9. Luster AD, Alon R, von Andrian UH. Immune cell migration in inflammation: present and future therapeutic targets. Nat Immunol. 2005; 6:1182–1190. [PubMed: 16369557]
10. Oxenius A, Bachmann MF, Zinkernagel RM, Hengartner H. Virus-specific MHC-class II-restricted TCR-transgenic mice: effects on humoral and cellular immune responses after viral infection. Eur J Immunol. 1998; 28:390–400. [PubMed: 9485218]
11. Selin LK, Lin MY, Kraemer KA, Pardoll DM, Schneck JP, Varga SM, Santolucito PA, Pinto AK, Welsh RM. Attrition of T cell memory: selective loss of LCMV epitope-specific memory CD8 T cells following infections with heterologous viruses. Immunity. 1999; 11:733–742. [PubMed: 10626895]
12. Fulton RB, Meyerholz DK, Varga SM. $Foxp3^+$ CD4 regulatory T cells limit pulmonary immunopathology by modulating the CD8 T cell response during respiratory syncytial virus infection. J Immunol. 2010; 185:2382–2392. [PubMed: 20639494]
13. Fulton RB, Olson MR, Varga SM. Regulation of cytokine production by virus-specific CD8 T cells in the lungs. J Virol. 2008; 82:7799–7811. [PubMed: 18524828]
14. Olson MR, Varga SM. CD8 T cells inhibit respiratory syncytial virus (RSV) vaccine-enhanced disease. J Immunol. 2007; 179:5415–5424. [PubMed: 17911628]

15. Oxenius A, Bachmann MF, Ashton-Rickardt PG, Tonegawa S, Zinkernagel RM, Hengartner H. Presentation of endogenous viral proteins in association with major histocompatibility complex class II: on the role of intracellular compartmentalization, invariant chain and the TAP transporter system. Eur J Immunol. 1995; 25:3402–3411. [PubMed: 8566030]
16. Varga SM, Wissinger EL, Braciale TJ. The attachment (G) glycoprotein of respiratory syncytial virus contains a single immunodominant epitope that elicits both Th1 and Th2 $CD4^+$ T cell responses. J Immunol. 2000; 165:6487–6495. [PubMed: 11086089]
17. Varga SM, Wang X, Welsh RM, Braciale TJ. Immunopathology in RSV infection is mediated by a discrete oligoclonal subset of antigen-specific $CD4^+$ T cells. Immunity. 2001; 15:637–646. [PubMed: 11672545]
18. Castilow EM, Olson MR, Meyerholz DK, Varga SM. Differential role of gamma interferon in inhibiting pulmonary eosinophilia and exacerbating systemic disease in fusion protein-immunized mice undergoing challenge infection with respiratory syncytial virus. J Virol. 2008; 82:2196–2207. [PubMed: 18094193]
19. Weiss KA, Christiaansen AF, Fulton RB, Meyerholz DK, Varga SM. Multiple CD4+ T Cell Subsets Produce Immunomodulatory IL-10 During Respiratory Syncytial Virus Infection. Journal of immunology. 2011
20. Srinivasan A, Foley J, McSorley SJ. Massive number of antigen-specific CD4 T cells during vaccination with live attenuated Salmonella causes interclonal competition. J Immunol. 2004; 172:6884–6893. [PubMed: 15153507]
21. Kamperschroer C, Quinn DG. Quantification of epitope-specific MHC class-II-restricted T cells following lymphocytic choriomeningitis virus infection. Cell Immunol. 1999; 193:134–146. [PubMed: 10222055]
22. Whitmire JK, Asano MS, Murali-Krishna K, Suresh M, Ahmed R. Long-term CD4 Th1 and Th2 memory following acute lymphocytic choriomeningitis virus infection. J Virol. 1998; 72:8281–8288. [PubMed: 9733872]
23. Varga SM, Welsh RM. Detection of a high frequency of virus-specific $CD4^+$ T cells during acute infection with lymphocytic choriomeningitis virus. J Immunol. 1998; 161:3215–3218. [PubMed: 9759834]
24. Cauley LS, Cookenham T, Miller TB, Adams PS, Vignali KM, Vignali DA, Woodland DL. Cutting edge: virus-specific $CD4^+$ memory T cells in nonlymphoid tissues express a highly activated phenotype. J Immunol. 2002; 169:6655–6658. [PubMed: 12471092]
25. Harrington LE, Most RRv, Whitton JL, Ahmed R. Recombinant vaccinia virus-induced T-cell immunity: quantitation of the response to the virus vector and the foreign epitope. J Virol. 2002; 76:3329–3337. [PubMed: 11884558]
26. Okumura M, Fujii Y, Inada K, Nakahara K, Matsuda H. Both $CD45RA^+$ and $CD45RA^-$ subpopulations of $CD8^+$ T cells contain cells with high levels of lymphocyte function-associated antigen-1 expression, a phenotype of primed T cells. J Immunol. 1993; 150:429–437. [PubMed: 7678274]
27. Andersson EC, Christensen JP, Marker O, Thomsen AR. Changes in cell adhesion molecule expression on T cells associated with systemic virus infection. J Immunol. 1994; 152:1237–1245. [PubMed: 7507962]
28. Harrington LE, Janowski KM, Oliver JR, Zajac AJ, Weaver CT. Memory CD4 T cells emerge from effector T-cell progenitors. Nature. 2008; 452:356–360. [PubMed: 18322463]
29. Gamadia LE, Rentenaar RJ, van Lier RA, ten Berge IJ. Properties of $CD4^+$ T cells in human cytomegalovirus infection. Hum Immunol. 2004; 65:486–492. [PubMed: 15172448]
30. Ewing C, Topham DJ, Doherty PC. Prevalence and activation phenotype of Sendai virus-specific $CD4^+$ T cells. Virology. 1995; 210:179–185. [PubMed: 7540783]
31. Roman E, Miller E, Harmsen A, Wiley J, Von Andrian UH, Huston G, Swain SL. CD4 effector T cell subsets in the response to influenza: heterogeneity, migration, and function. J Exp Med. 2002; 196:957–968. [PubMed: 12370257]
32. Yang CP, Sparshott SM, Duffy D, Garside P, Bell EB. The phenotype and survival of antigen-stimulated transgenic CD4 T cells in vivo: the influence of persisting antigen. Int Immunol. 2006; 18:515–523. [PubMed: 16481344]

33. Whitmire JK, Benning N, Whitton JL. Precursor frequency, nonlinear proliferation, and functional maturation of virus-specific $CD4^+$ T cells. J Immunol. 2006; 176:3028–3036. [PubMed: 16493061]

34. Kleinewietfeld M, Starke M, Di Mitri D, Borsellino G, Battistini L, Rotzschke O, Falk K. CD49d provides access to “untouched” human $Foxp3^+$ Treg free of contaminating effector cells. Blood. 2009; 113:827–836. [PubMed: 18941119]

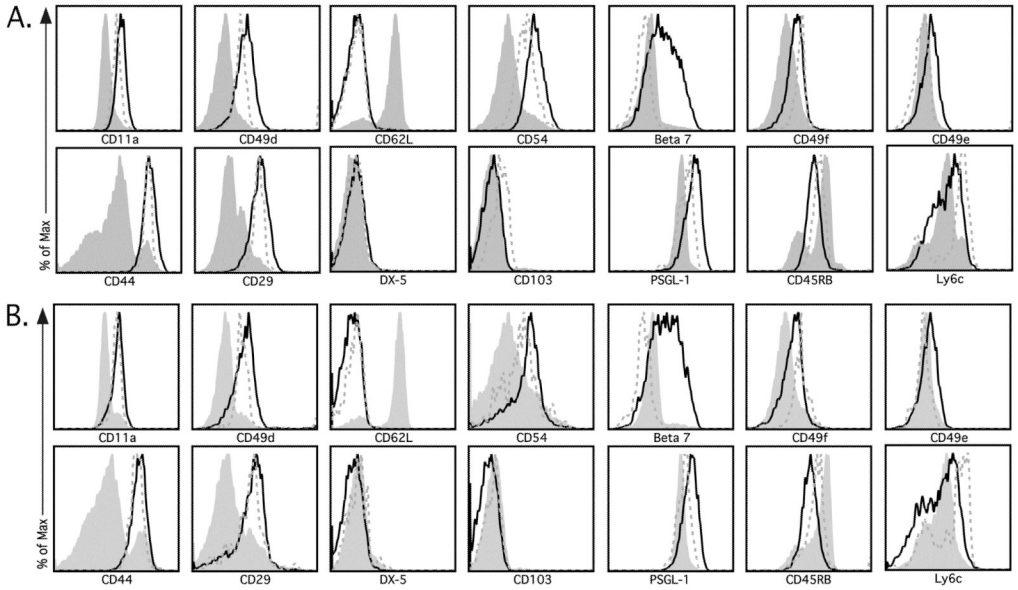

Figure 1.

Identification of markers that distinguish Ag-specific CD4 T cells. Thy1.1 SMARTA CD4 T cells were transferred into naïve Thy1.2 C57BL/6 mice, followed by i.n. infection with LCMV 24 h later. (A) Spleens and (B) lungs were harvested at day 8 (black line) and 30 (dashed grey line) post-infection. Representative plots depict cell surface expression of either CD11a, CD49d, CD44, CD29, CD62L, CD54, β_7 integrin, CD49f, CD49e, CD49b (DX-5), CD103, PSGL-1, CD45RB or Ly6C on SMARTA CD4 T cells ($CD4^+Thy1.1^+$). Surface marker expression on CD4 T cells from the naïve SMARTA donor mouse (shaded grey line) is also shown. Similar results were obtained from 4 independent experiments with 3–4 mice per group.

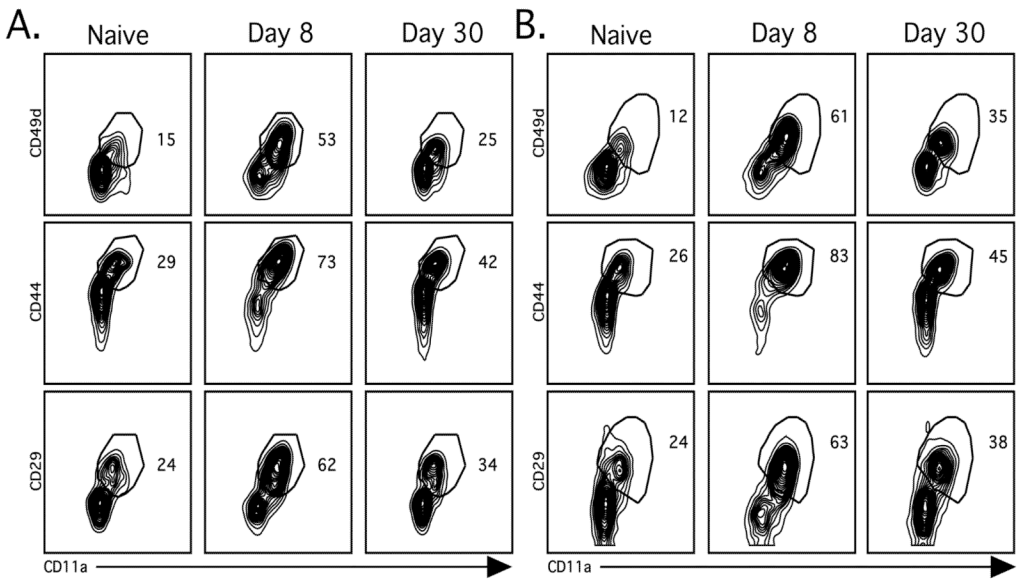

Figure 2.

Identification of surface markers that distinguish endogenous Ag-specific CD4 T cells. (A) Spleens and (B) lungs were harvested from naïve or LCMV-infected mice as described in Figure 1. Representative plots depict cell surface expression patterns of CD11a in combination with either CD49d, CD29 or CD44 on endogenous CD4 T cells ($CD4^{+}Thy1.1^{-}$). Similar results were obtained from 4 independent experiments with 3–4 mice per group.

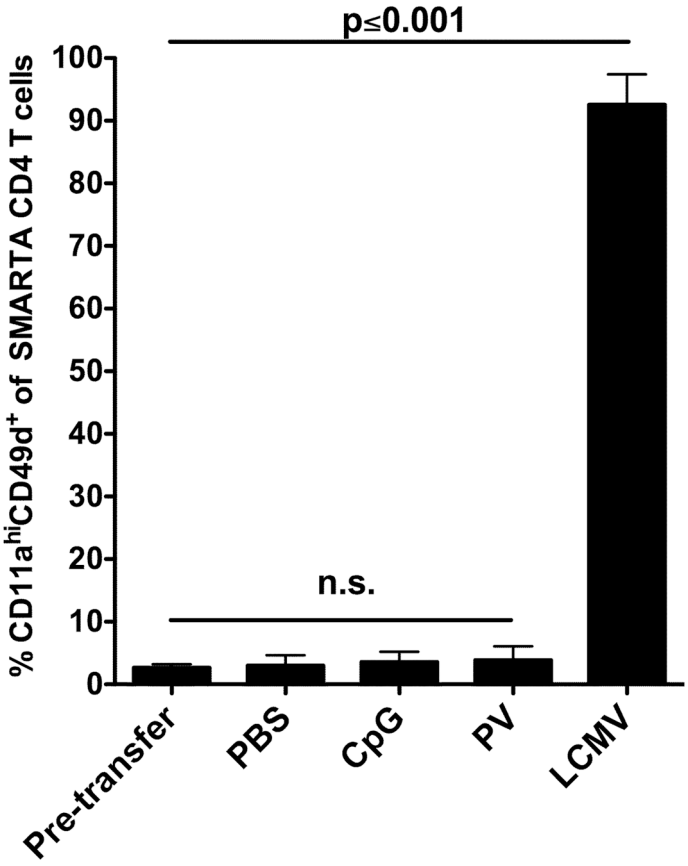

Figure 3.

Non-specific inflammatory mediators do not modulate CD11a CD49d cell surface expression. Thy1.1 LCMV-Tg SMARTA CD4 T cells were transferred into Thy1.2 C57BL/6 mice and 24 h later mice were administered either PBS, CpG, PV or LCMV i.p. Spleens were harvested at day 8 post-infection and SMARTA CD4 T cells ($CD4^+Thy1.1^+$) were analyzed for cell surface expression pattern of CD11a and CD49d. Combined results are shown from 3 independent experiments with an *n*=3 mice per group. Error bars represent the SD. Data were analyzed using unpaired t tests.

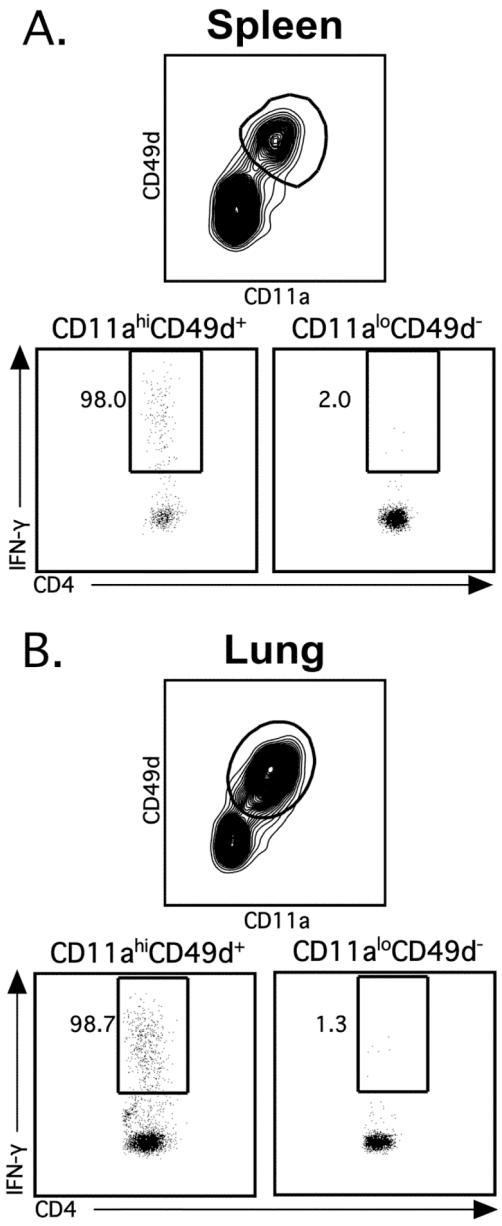

Figure 4.

Ag-specific effector CD4 T cells are CD11a^{hi}CD49d^{+}. C57BL/6 mice were infected i.n. with LCMV and (A) spleens and (B) lungs were harvested at day 8 post-infection. CD4 T cells were incubated in BFA alone or stimulated with the LCMV-derived peptide $GP_{66–80}$. Representative staining depicts IFN-γ production by CD4^{+}CD90.2^{+} T cells gated on either CD11a^{hi}CD49d^{+} (left) or CD11a^{lo}CD49d$^{−}$ (right). Numbers denote the percentage of IFN-γ^{+} CD4 T cells that are either CD11a^{hi}CD49d^{+} or CD11a^{lo}CD49d$^{−}$. Similar results were obtained from 4 independent experiments with 3–4 mice per group.

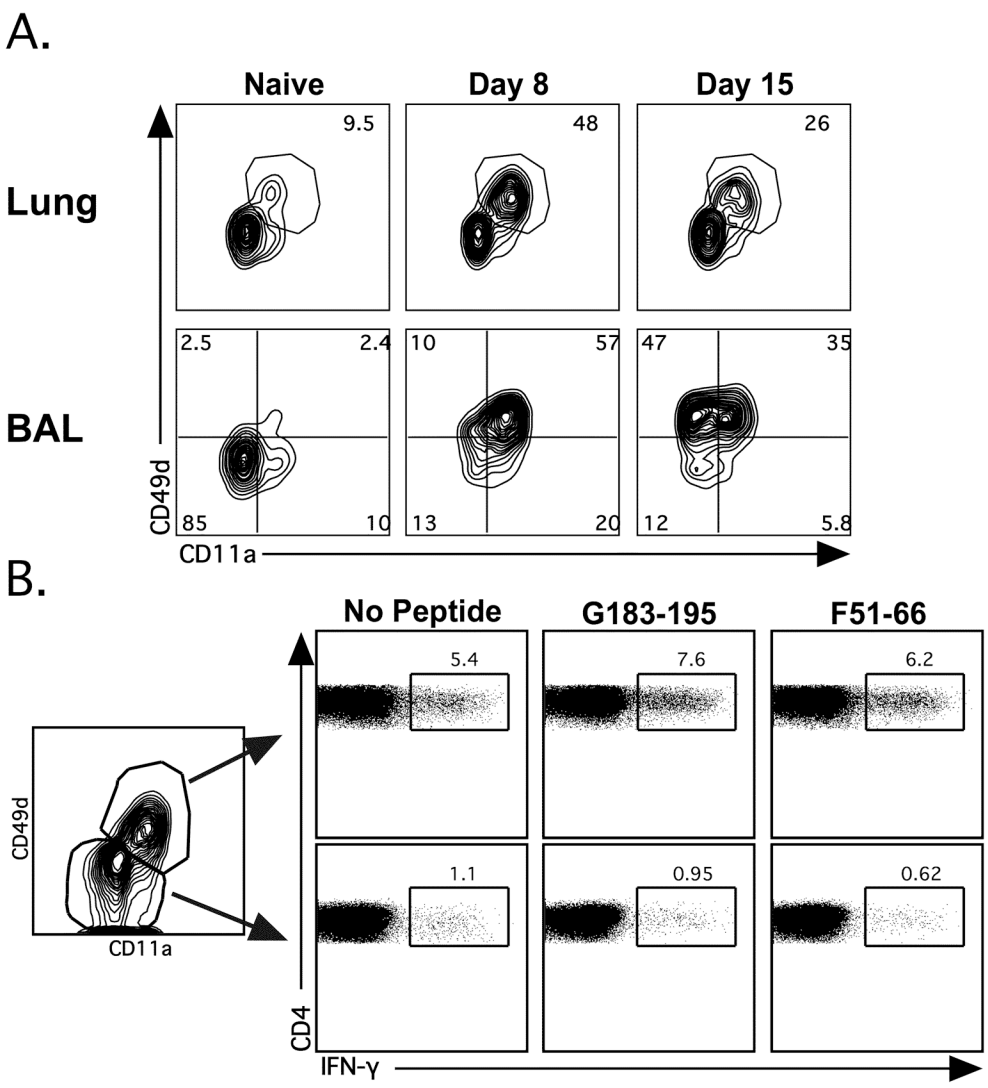

Figure 5.

CD11a and CD49d identify Ag-specific CD4 T cells following acute RSV infection. BALB/c mice were infected with RSV i.n.. (A) Representative plots depict CD11a and CD49d expression on lung and BAL $CD4^{+}Thy1.2^{+}$-gated CD4 T cells at day 8 and 15 post-infection. (B) Lung CD4 T cells from day 8 RSV infected BALB/c mice were incubated in BFA alone or stimulated with either the RSV peptide $G_{183–196}$ or $F_{51–66}$. Representative plots depict IFN-γ production between $CD11a^{lo}CD49d^{-}$ (top) and $CD11a^{hi}CD49d^{+}$ (bottom) CD4 T cells ($CD4^{+}CD90.2^{+}$). Similar results were obtained from 4 independent experiments with 3–4 mice per group.

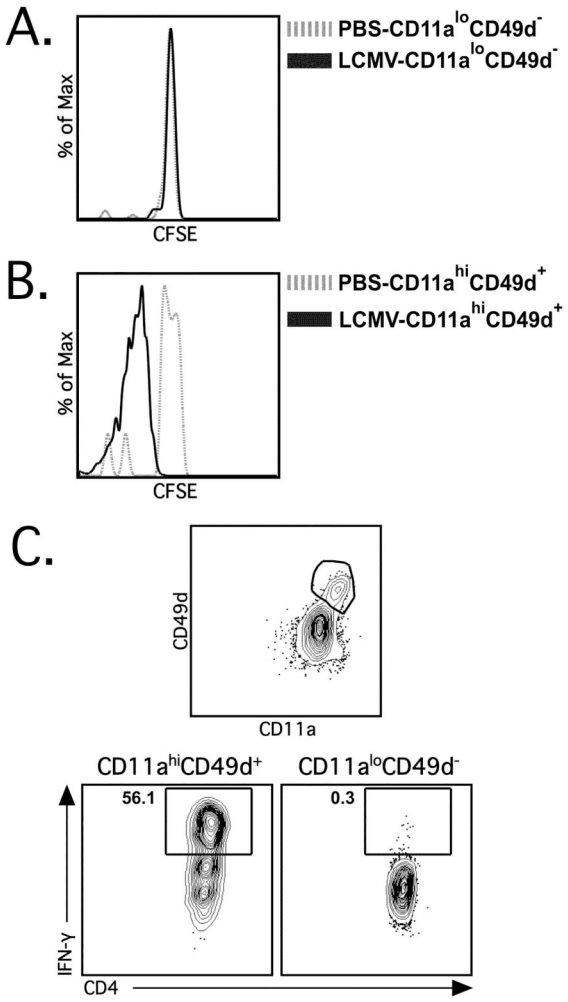

Figure 6.

Memory CD4 T cells are CD11a^{hi}CD49d^{+}. (A) CD11a^{lo}CD49d^{-} and (B) CD11a^{hi}CD49d^{+} CD4 T cells (CD4^{+}CD90.1^{+}) were sorted from LCMV-immune (i.e. day ≥60 post-LCMV infection) CD45.1 congenic mice, labeled with CFSE and transferred into naïve CD45.2 C57BL/6 mice. Recipient mice were subsequently administered either PBS (dashed grey line) or LCMV (solid black line) i.p. and spleens were harvested at day 4 post-infection. Representative plots show CFSE dilution profiles of transferred CD11a^{hi}CD49d^{+} CD4 T cells (left) and CD11a^{lo}CD49d^{-} CD4 T cells (right) from mice administered PBS (dashed grey line) or LCMV (solid black line). Similar results were obtained from 3 independent experiments with 3–4 mice per group. (C) PBL were obtained from LCMV-immune mice and the CD4 T cells were incubated in either BFA alone or stimulated with PMA/Ionomycin. Representative staining depicts IFN-γ production by CD4^{+}CD90.2^{+} T cells gated on either CD11a^{hi}CD49d^{+} (left) or CD11a^{lo}CD49d^{-} cells (right). Numbers denote the percentage of IFN-γ^{+} CD4 T cells within each respective population. Similar results were obtained from 2 independent experiments with 3–4 mice per group.

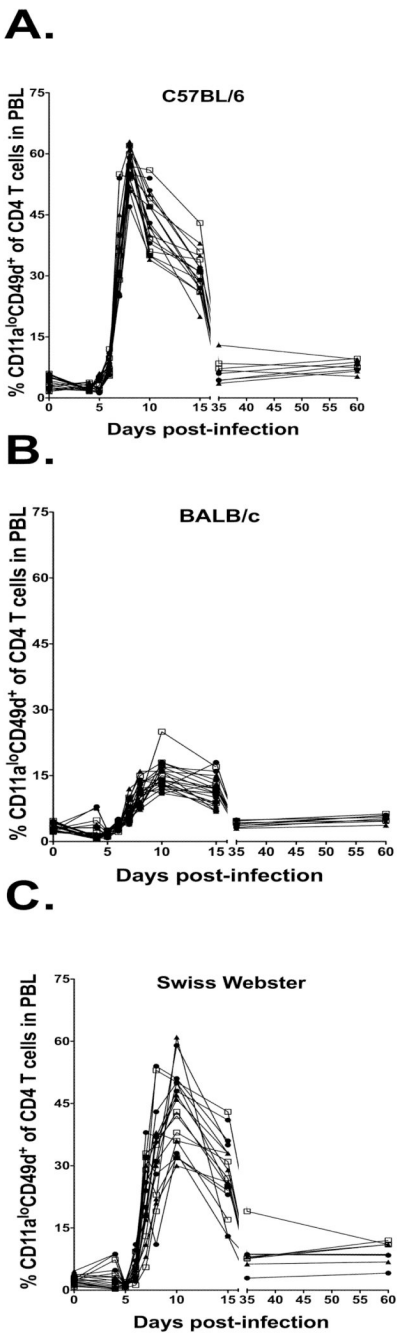

Figure 7.

Tracking the kinetics and magnitude of the total LCMV-specific CD4 T cell response following infection. C57BL/6, BALB/c and Swiss Webster mice were infected i.p. with LCMV and PBL were obtained at 0, 4, 5, 6, 7, 8, 10, 15, 35 and 60 days post-infection. Percentage of $CD11a^{hi}CD49d^{+}$ CD4 T cells ($CD4^{+}CD90.2^{+}$) was examined in (A) C57BL/6, (B) BALB/c and (C) Swiss Webster mice. Combined results are shown from 2 independent experiments with an n=17–18 mice per group.

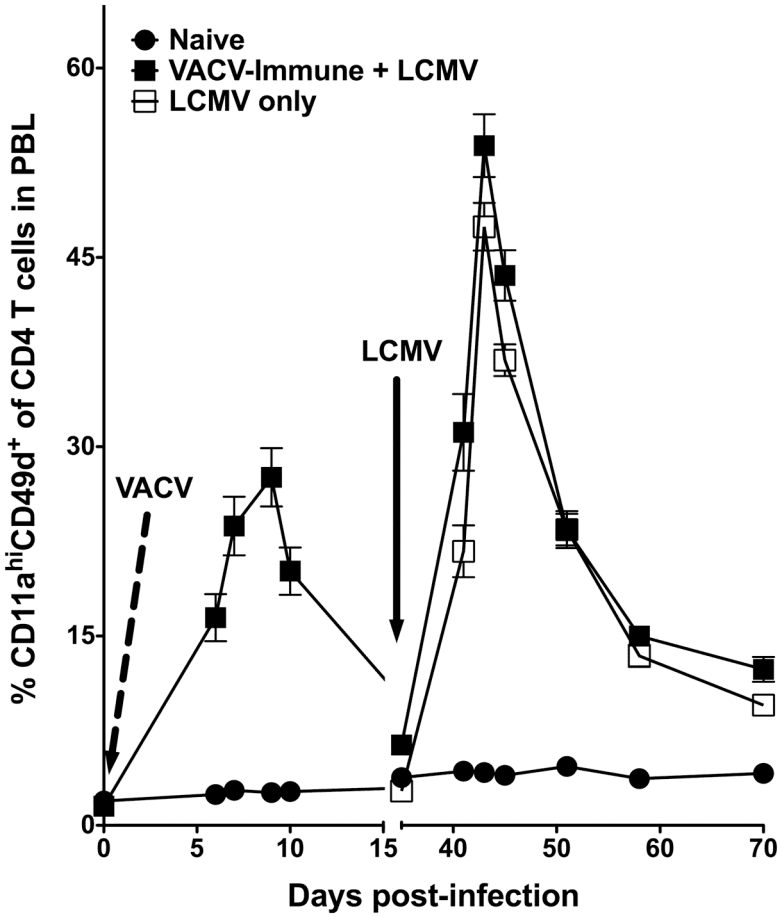

Figure 8.

Tracking newly generated Ag-specific CD4 T cells following heterologous infection. C57BL/6 mice were infected i.p. on Day 0 with VACV (dashed line) and PBL was obtained at the indicated days post-infection and the frequency of $CD11a^{hi}CD49d^{+}$ CD4 T cells ($CD4^{+}CD90.2^{+}$) was examined. At day 35 post-infection, these mice and naïve mice were infected with LCMV i.p. (black arrow) and PBL was obtained at the indicated days post-infection and the percentage of $CD11a^{hi}CD49d^{+}$ CD4 T cells ($CD4^{+}CD90.2^{+}$) was examined. Combined results are shown from 2 independent experiments with an n=7–8 mice per group. Error bars represent the SEM.